Journal of Structural Geology, Vol. 10, No. 1, pp. 101 to 108, 1988
Printed in Great Britain

0191-8141/88 $03.00 + 0.00
Pergamon Press plc

An automated machine for pure shear deformation of analogue materials in plane strain

NEIL S. MANCKTELOW

Geologisches Institut, ETH-Zentrum, CH-8092 Zürich, Switzerland

(*Received* 28 *August* 1986; *accepted in revised form* 23 *June* 1987)

Abstract—A plane strain, pure shear rig has been developed for the deformation of rock-analogue materials under tightly controlled experimental conditions. Shortening of up to 42% is possible, with constant natural strain rates and a predetermined confining side stress (σ_3). Differential stress, side stress, temperature and strain rate are recorded during the experiments, allowing rheological calibration under exactly the same conditions used in the applied studies of mechanical instabilities (folds, boudinage, etc.). The relatively large specimen size, three-piece side plate design and the extensive use of low-friction facing materials in contact with the model result in boundary conditions which closely approximate plane strain, pure shear.

INTRODUCTION

AVERAGE geological strain rates are very slow, with deformation phases commonly involving time spans in the range of 10^5–10^7 years (e.g. Pfiffner & Ramsay 1982, fig. B1). Short-term events within this broader time scale may be observed directly (e.g. earthquakes), but the accumulation of significant finite strain during continuing deformation is clearly beyond the realm of direct observation. The progressive development of deformational structures can be investigated indirectly, however, by observing presumed intermediate stages in the field and by modelling studies. There are three alternative approaches to modelling rock deformation:

(1) rock mechanics experiments using natural or synthetic rock materials (cf. the review of Tullis & Tullis 1986);

(2) mathematical modelling (e.g. Biot 1961, 1965, Ramberg 1963, Dieterich & Carter 1969, Parrish 1973);

(3) scale modelling using analogue materials (e.g. Hudleston 1973, Cobbold 1975a, b).

All of these modelling methods require major extrapolations for comparison with the natural examples.

Rock mechanics experiments on single crystals and polycrystalline natural or synthetic rocks have the clear advantage that both the phenomenological and micromechanical models deduced are directly relevant to a geological material, *if* the deformation mechanisms in the laboratory and nature are the same. The problem is that the necessary extrapolation from experimental to geological conditions is very large (for strain rate usually around seven orders of magnitude, Paterson 1987). For the study of deformational structures (folds, boudins, etc.), the experimental samples are generally too small, boundary effects too great (e.g. significant barrelling of the sample) and the strain geometry (axial shortening, Flinn parameter $k = 0$) unrealistic (cf. Tullis & Tullis 1986). There is also no facility for observing the development of structures (only the initial and final states can be examined) or for measuring incremental and finite strains within the deforming sample (with the notable exception of the split cylinder experiments of Spiers 1979).

Mathematical modelling does not suffer from machine constraints and allows the continued and detailed monitoring of developing structures. However, it is limited in its complexity by the necessity for either an analytical solution or by the amount of computer time which can be invested in an iterative solution (if a unique solution exists). The models must therefore be simplified. This is commonly done by choosing simple material properties (linear elastic or linear viscous) and boundary conditions. Often only the initiation of structures is considered, as the model assumptions are inappropriate for finite amplitudes (e.g. Biot 1961, Ramberg 1963, Fletcher 1974, Smith 1977).

Scale modelling using analogues of rock materials (e.g. paraffin wax, clay, silicone putty) provide the third alternative. The basic theory of scale models and their application to geological problems was thoroughly discussed by Hubbert (1937). Provided that: (i) strain rates are slow (i.e. inertial forces are negligible); (ii) body forces (gravity) can be ignored; and (iii) the rheology of the analogue substance is similar to that of the rock to be modelled (cf. Cobbold 1975b, Weijermars & Schmeling 1986), geometrical, kinematic and dynamic similarity can be obtained. As with rock mechanics studies, machine and material constraints are a major consideration when designing scale models. Models should be large enough to keep boundary effects away from the region of interest, but they cannot be too large or the forces required for deformation become impractically large. If the stress–strain history is to be recorded, then the frictional forces must be as low as possible. This places a limit on the strength and rigidity of the machine; massive machines generally produce more friction, while a flimsy machine cannot support the forces required for deformation of the model.

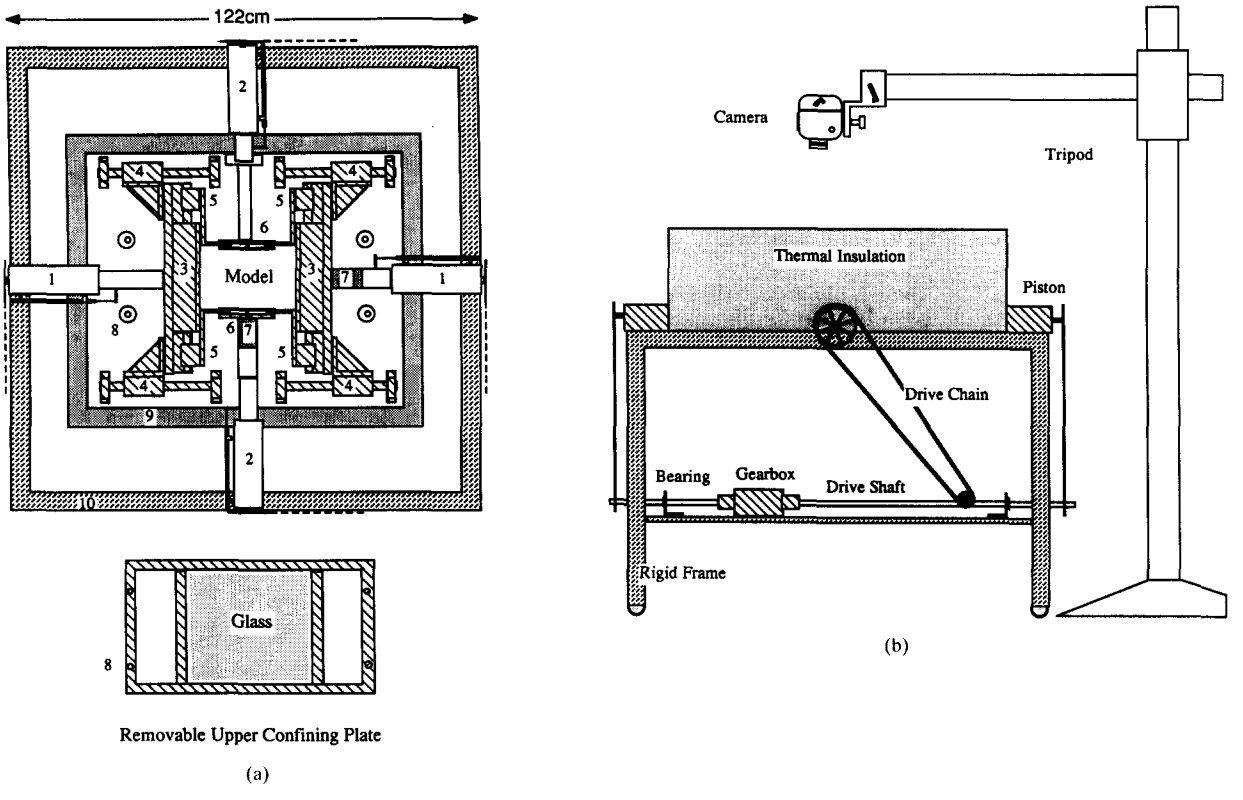

Fig. 1. (a) Plan view of the plane strain, pure shear machine with the upper confining plate removed. 1: Compression piston with displacement transducer; 2: confining piston with displacement transducer; 3: compression plates faced with 5 mm Teflon sheet; 4: linear bearing for the compression plates which run on a stainless steel bar; 5: linear bearing for the side plates. The runner bar is mounted on the compression plate assembly 3; 6: three-piece side plate assembly. The central section is notched onto the confining piston 2 and remains stationary relative to this piston; 7: force transducer with a range of 0–5000 N; 8: anchoring points for the upper confining plate; 9: thermal insulation 5 cm thick surrounding the whole rig; 10: rigid frame for the rig. (b) Side view of the pure shear rig, with the thermal insulation box and camera in place.

MACHINE GEOMETRY

Over the last 4 years, a machine for the deformation of analogue materials during pure shear, plane strain has been developed, so as to meet the rather strict requirements of controlled scale model experiments. The machine of Cobbold (1975a) was a first step in this direction but was not capable of imposing a confining pressure. The rig used by Neurath & Smith (1982), in an excellent series of fold and boudinage experiments, was capable of maintaining a confining pressure (of *ca* 1 bar = 0.1 MPa) but was unsuitable for the direct measurement of stress and strain during the experiments, due to the large frictional forces.

The newly designed machine basically consists of two sets of plates mounted on linear roller bearings (Fig. 1). The compression plates use linear bearings riding on stainless steel bars fixed directly onto the rigid base plate. The bearings for the side plates are attached to the compression plates themselves. The base plate and surfaces of the compression plates are faced with 5 mm thick Teflon sheets to reduce friction. The side plates are a three-piece construction such that the unavoidable overlap of the plates occurs away from the region of interest in the centre of the model. Initial model dimensions are usually 29 cm long × 12 cm wide × 6 cm thick. Wider specimens may be used, but this then limits the maximum shortening which can be achieved. With the present side-plate geometry, an absolute maximum of around 42% shortening is possible. The upper confining plate (Fig. 1a) consists of optical-quality plate glass, 1 cm thick, mounted in a strengthened tubular steel frame. This allows continuous observation of the upper surface of the model.

The advance of the compression plates and the retraction of the side plates is controlled by worm-screw pistons driven, via a chain drive and reduction gears, by two three-phase motors with a speed range of 100:1. The speed of the motors is tightly controlled using a DC tachometer and can be varied using a 0–10 V DC signal output from the control computer. Rubber drive belts between the motors and the gearbox train reduce wear on the gears during rapid motor acceleration. The run/stop state and the direction of motor rotation, and therefore the advance or retraction of the drive pistons, is controlled by relays via digital output lines from the computer. Four of these lines are used to drive an LCD display on the front surface of the model which shows the per cent shortening during experiments. The relay switching between up to four temperature probes placed against the sides of the model block is also controlled over these digital lines.

EXPERIMENT CONTROL

The experiments are run under closed-loop computer control, currently based on a DEC LSI-11/2 mini-computer system. Forces on the compression and side plates are detected by two force transducers (0–5000 N) and the dimensions of the model by four linear displacement transducers. Values are intermittently digitized by an integrating digital voltmeter and passed to the computer under program control. This technique is relatively slow, but eliminates noise better than does analogue to digital conversion by continuous approximation, as provided by many 'plug-in' interface cards.

Strain rate

Experiments are run at a constant strain rate, $\dot{\varepsilon} = \partial\varepsilon/\partial t$, where ε is the natural or logarithmic strain. This requires that the displacement rate of the compression pistons, $\partial X/\partial t$, is proportional to the current specimen length. In practice, a closed-loop control of the average strain rate is maintained, requiring minor correction of the compression piston speed. At sampling time T, for a constant average natural strain rate $\dot{\varepsilon}$, the required length of the specimen is given by:

$$X_r = X_0 \exp(\dot{\varepsilon}T).$$

However, the actual measured length at time T is X_a, giving an error

$$X_d = X_a - X_r.$$

An attempt is made to correct this error within the next four sampling intervals by changing the theoretical piston speed by an amount given by $X_d/(4T_d)$, where T_d is the time delay between sampling events. For subsequent sampling events, the correction factor is not altered unless the absolute difference between the measured and required specimen length increases or if its sign changes. This technique introduces the required damping effect for stable motor speed. Without such damping, motor speeds can oscillate wildly, resulting in unnecessary wear to the whole drive train. The closed-loop control is capable of maintaining a preset strain rate to within less than ±0.2% (e.g. 3.00×10^{-5} s^{-1} of Fig. 3).

Confining stress

The dimensions of one of the side plates and the force it exerts on the restraining piston are monitored by the computer and the speed of the motor driving the confining pistons varied in order to maintain a constant confining side stress (with a current upper limit of *ca* 1.5 bar). The necessary control algorithm is derived in the Appendix; the damped correction method is in principle similar to that for strain rate control. As the confining stress control is a more sensitive process, however, the sampling interval is kept shorter than for strain rate control and data collection. The control program loops on the confining stress routine, branching occasionally to collect data and monitor the strain rate.

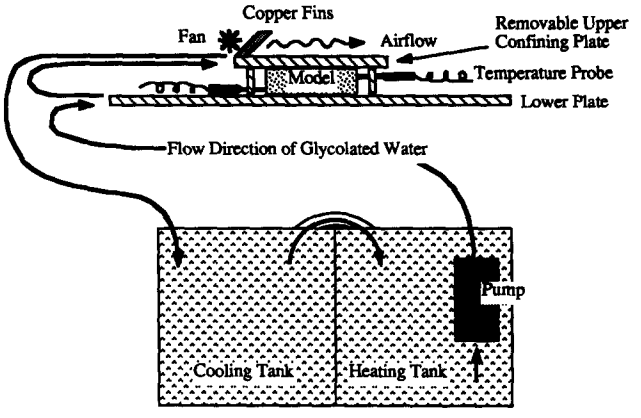

Fig. 2. Stylized diagram of the temperature control circuit. The lower aluminium plate contains imbedded copper coils through which the water is pumped. The upper unit consists of a glass plate mounted in a hollow tubular steel frame, through which the water is also pumped. A transverse fan blows air through copper fins attached to this frame across the upper surface of the glass plate.

Temperature

The activation energy for the deformation of paraffin wax, the analogue material most commonly used in this laboratory, is very high (>120 kcal mole^{-1}, Mancktelow in press) under the experimental conditions. In other words, the deformation behaviour is very temperature dependent. The temperature during the experimental runs must be held constant and should show little variation across the model. This has been achieved by using pumped glycolated water as shown in Fig. 2. Two 30 l reservoirs are used, one with a refrigerating circuit and one with a heating circuit. The thermostat of the cooling system is set *ca* 0.5°C higher than that of the heating circuit. The water is pumped through copper coils welded into the base plate and then through the tubular steel frame holding the upper glass plate before returning to the reservoir. A transverse fan blows air through copper fins connected to the tubular frame and across this upper plate. The whole working area of the machine is encased in a 5 cm thick plastic foam insulating box with a plexiglass upper surface to allow observation. Accurately calibrated temperature probes on each side plate indicate a temperature difference of <0.2°C over an operating range of 0–40°C. Models are cooled *in situ* before removal after an experiment to eliminate the possibility of induced deformation during handling.

DATA COLLECTION

During the course of the experiment the natural strain, engineering strain, differential stress ($\sigma_1 - \sigma_3$), side stress (σ_3), temperature and time (seconds since experiment start) are recorded by the computer on a hard disk data file. Several of these parameters are also displayed graphically on the terminal screen during the run. The display format depends on the type of experiment selected. If a constant strain rate is required, then the differential stress, side stress and strain rate are

plotted against per cent shortening. If a relaxation test is requested, then differential stress and side stress are displayed against time.

The strain on the upper surface of the model can be monitored with a closely-spaced, rectangular grid. This is currently achieved by inscribing narrow grooves *ca* 0.5 mm deep within the upper surface of the paraffin wax block, spraying with a quick-drying black paint and, after drying, carefully scraping the upper surface until only a fine grid remains, preserved within the grooves. This slightly recessed grid is then less susceptible to contact effects against the upper glass plate during the confined deformation.

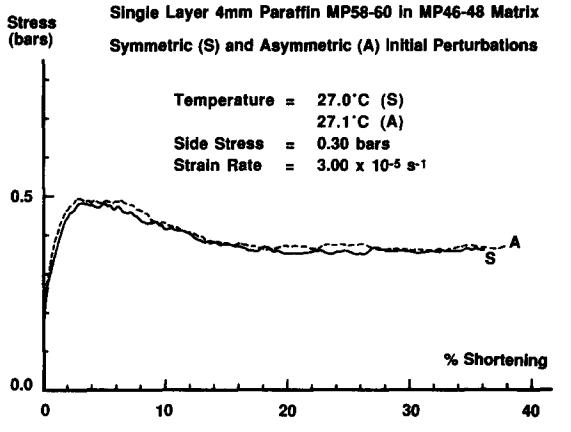

Fig. 3. Plot of differential stress ($\sigma_1 - \sigma_3$, 1 bar = 0.1 MPa) vs % shortening for the experiments of Fig. 4 (S: symmetric) and Fig. 5 (A: asymmetric). Under the experimental conditions, the matrix alone would flow in steady state at 0.35 bar (Mancktelow in press, Paraffin MP46–48 Batch No. 1), while the stiffer layer displays marked strain softening behaviour with an initial yield stress around 6.6 bar (i.e. *ca* 19 times the matrix flow stress).

PHOTOGRAPHY

Two forms of photography are used depending upon the aim of the experiment. For detailed scientific studies, 24 6 × 6 cm black and white photos are taken with a camera released automatically by a timer and synchronized with two flashlights. For teaching films, a similar arrangement with a 16 mm colour movie camera is used, with a time interval such that a single experiment (say 5 h) occupies 1.5 min of film time at 25 frames s^{-1}.

ANALYSIS OF COLLECTED DATA

For constant strain rate, the differential stress is plotted against per cent shortening. The simple averages of temperature and of the side stress are determined. A linear regression of natural strain against time gives the average strain rate. For relaxation test data a smoothing technique using cubic splines is employed to determine the gradient along the relaxation curve, which is then plotted on a $\log_e$–$\log_e$ scale against stress. This approach is essential, as minor errors in the original data or in the reading of recorded data (e.g. when digitizing a continuous relaxation curve from a chart recorder) can result in significant inaccuracies in the determined slope of the curve.

The photographically recorded deformed grids on the upper surface of the model are digitized and the resulting data files used to determine the distribution of the finite strain, incremental strain between any two stages, perturbation strain (strain additional to that applied to the boundaries, and therefore due to internal instabilities), rotation, displacement paths of material points and so on.

APPLICATIONS

The deformation rig was designed to investigate the development of mechanical instabilities using rock analogues under carefully controlled experimental conditions. Specific fields of current interest include the initiation and propagation of shear zones (Baumann 1986, Baumann & Mancktelow 1987), the dominant wavelength, initial amplification rates and development with increasing strain of low competence contrast single- and multi-layer folds and boudins (cf. Cobbold 1975b, Neurath & Smith 1982), and the effect of initial perturbation geometry on fold geometry and development (Cobbold 1975b, Abbassi & Mancktelow work in preparation). The results of these on-going studies will be discussed in detail elsewhere. However, some of the data from two experiments of Abbassi & Mancktelow (work in preparation) are presented in Figs. 3–6, to demonstrate the capabilities of the deformation rig. It is clear from Fig. 3 that the reproducibility of the stress–strain curves is excellent, and is apparently independent of the initial symmetry of the perturbation. Despite the low flow stresses involved, the combined noise (both electronic and mechanical, e.g. from the tendency for frictional stick–slip of the bearings and over-riding surfaces) is minimal. Photographic records, as in Figs. 4 and 5, provide the raw data to calculate the finite-strain distribution from which, for example, a plot of the orientation and length of the long axes of the strain ellipses can be generated (Fig. 6). The trajectories determined from such a plot may correspond to the cleavage patterns in natural rocks, a possibility which can be checked by reference to field examples.

It should be clear from this brief example that analogue experiments, in which the stress–strain history at the boundaries and the geometry of the strain distribution about the instability are monitored throughout the development history, can add greatly to our understanding of naturally occurring structures.

CONCLUSION

The deformation machine described here has the following advantages for the study of the development of geological structures.

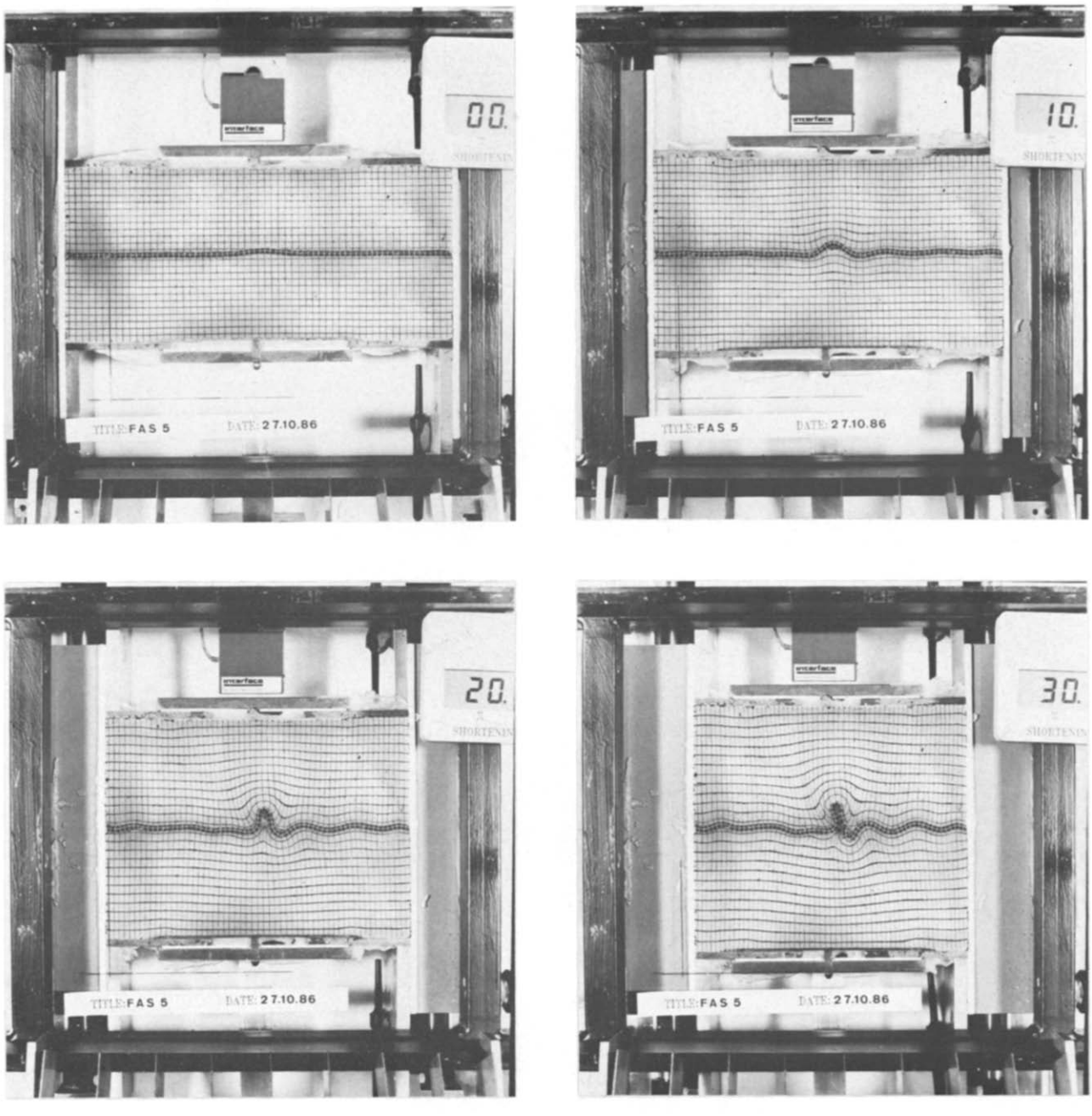

Fig. 4. Photographs at 0, 10, 20 and 30% shortening for a single-layer fold experiment with an introduced symmetric perturbation. The perturbation was initially arcuate, with an amplitude of 2.5 mm and limb dips of 6°. Prior to deformation, the model length was 29 cm, with a 4 mm thick single layer of stiffer paraffin wax (melting range 58–60°C) embedded within paraffin wax of melting range 46–48°C. Deformation was at a constant temperature of 27.0°C, under a confining stress of 0.3 bar, and with an imposed constant natural strain rate of 3.00×10^{-5} s^{-1} (cf. Fig. 3).

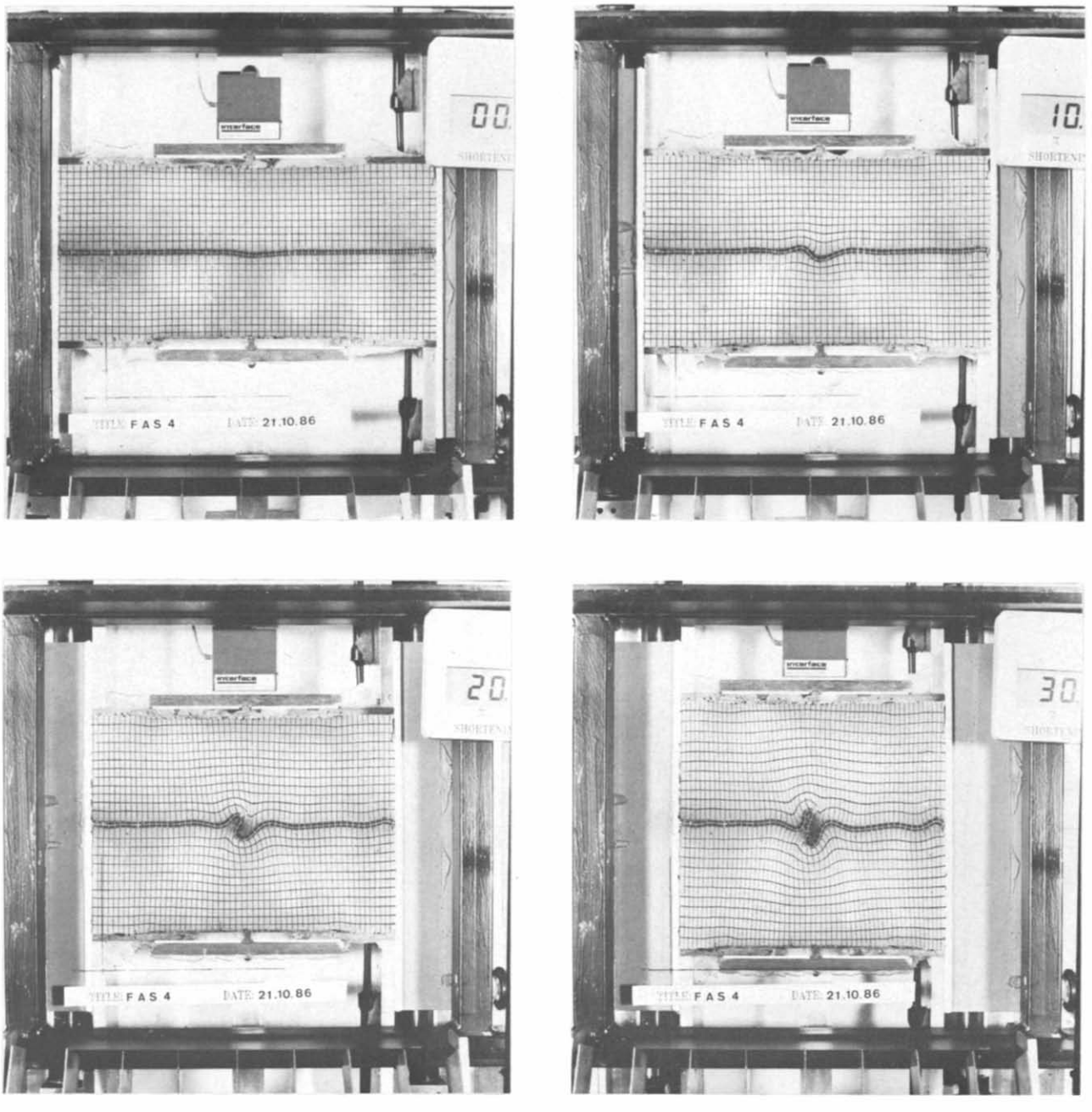

Fig. 5. Photographs at 0, 10, 20 and 30% shortening for a single-layer fold experiment which differs from that of Fig. 4 only in that the initial perturbation was asymmetric. The introduced irregularity has an amplitude of 2.3 mm, but differing limb dips of 4.5 and 8°, respectively.

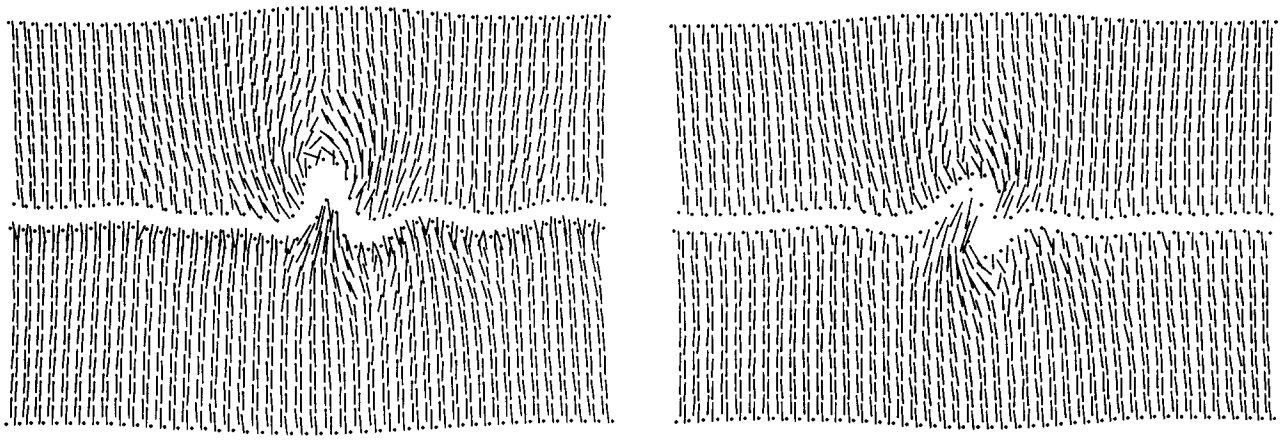

Fig. 6. Plots of the long axes of the finite-strain ellipses within the matrix for the symmetric and asymmetric model experiments at 23% shortening (cf. Figs. 4 and 5).

(a) Specimens are reasonably large (initially 29 × 12 × 6 cm). This is important if the zone of contact strain around developing instabilities is not to be truncated by the model boundaries, and also keeps unavoidable boundary effects well away from the central region of the model.

(b) The models are deformed under constant natural strain rate rather than constant piston displacement rate. This distinction becomes important for large finite strains.

(c) The strains (both finite and incremental) and particle displacement paths can be determined throughout the experiments from the photographic record of the inscribed grid.

(d) A closely-controlled confining pressure broadens the ductile field of the analogue materials and hinders the development of gaps, for example between matrix and layer on the inner arc of folds.

(e) The differential stress and strain can be accurately measured during the experiments. This allows the onset of the instability to be easily defined (change from nearly steady state to marked strain softening) and the strain-softening history during amplification of the instability to be studied. It also means that the rheology of the materials can be characterized under exactly the same conditions as hold in the experiments themselves (in contrast, for example, to the rig of Neurath & Smith 1982).

(f) The temperature is closely controlled and accurately measured.

(g) The three-piece design of the side plates and the extensive use of low-friction facing material (Teflon) reduces the edge and frictional effects to a minimum.

Acknowledgements—Many thanks are due to John Ramsay, who initiated the Model Deformation Laboratory project at the ETH-Zürich and has strongly supported it throughout, to Robert Hofmann who constructed many of the mechanical components and whose suggestions aided in its design, to Peter Cobbold who designed the screw jacks and rigid frame and to John Mott of Leeds University Earth Sciences Workshop who built them, to Sven Girsperger for much help and discussion on the computer control interface, and to Martin Casey, Peter Cobbold, Peter Hudleston, Stefan Schmid and David Olgaard for discussion and comment.

REFERENCES

Baumann, M. T. 1986. Verformungsverteilung an Scherzonenenden: Analogmodelle und natürliche Beispiele. Unpublished doctoral thesis, ETH-Zürich.

Baumann, M. T. & Mancktelow, N. S. 1987. Initiation and propagation of ductile shear zones (Abstract). *Terra cognita* **7**, 47.

Biot, M. A. 1961. Theory of folding of stratified viscoelastic media and its implications in tectonics and orogenesis. *Bull. geol. Soc. Am.* **72**, 1595–1620.

Biot, M. A. 1965. *Mechanics of Incremental Deformation*. John Wiley & Sons, New York.

Cobbold, P. R. 1975a. A biaxial press for model deformation and rheological tests. *Tectonophysics* **26**, T1–T5.

Cobbold, P. R. 1975b. Fold propagation in single embedded layers. *Tectonophysics* **27**, 333–351.

Dieterich, J. H. & Carter, N. L. 1969. Stress history of folding. *Am. J. Sci.* **267**, 129–154.

Fletcher, R. C. 1974. Wavelength selection in the folding of a single layer with power-law rheology. *Am. J. Sci.* **274**, 1029–1043.

Hubbert, M. K. 1937. Theory of scale models as applied to the study of geologic structures. *Bull. geol. Soc. Am.* **48**, 1459–1520.

Hudleston, P. J. 1973. An analysis of 'single layer' folds developed experimentally in viscous media. *Tectonophysics* **16**, 189–214.

Mancktelow, N. S. The rheology of paraffin wax and its usefulness as an analogue for rocks. *Bull. geol. Instn. Univ. Uppsala*. In press.

Neurath, C. & Smith, R. B. 1982. The effect of material properties on growth rates of folding and boudinage: experiments with wax models. *J. Struct. Geol.* **4**, 215–229.

Parrish, D. K. 1973. A nonlinear finite element fold model. *Am. J. Sci.* **273**, 318–334.

Paterson, M. S. 1987. Problems in the extrapolation of laboratory rheological data. *Tectonophysics* **133**, 33–43.

Pfiffner, O. A. & Ramsay, J. G. 1982. Constraints on geological strain rates: arguments from finite strain states of naturally deformed rocks. *J. geophys. Res.* **87**, 311–321.

Ramberg, H. 1963. Fluid dynamics of viscous buckling, applicable to folding of layered rocks. *Bull. Am. Ass. Petrol. Geol.* **47**, 484–515.

Smith, R. B. 1977. Formation of folds, boudinage and mullions in non-Newtonian materials. *Bull. geol. Soc. Am.* **88**, 312–320.

Spiers, C. J. 1979. Fabric development in calcite polycrystals deformed at 400°C. *Bull. Minéral.* **102**, 282–289.

Tullis, T. E. & Tullis, J. 1986. Experimental rock deformation techniques. In: *Mineral and Rock Deformation: Laboratory Studies. The Paterson Volume* (edited by Hobbs, B. E. & Heard, H. C.). *Am. Geophys. Un. Monograph* **36**, 297–324.

Weijermars, R. & Schmeling, H. 1986. Scaling of Newtonian and non-Newtonian fluid dynamics without inertia for quantitative modelling of rock flow due to gravity (including the concept of rheological similarity). *Phys. Earth & Planet. Interiors* **43**, 316–330.

APPENDIX

The side stress algorithm

The algorithm used to maintain a constant side stress σ_3 is based on the following:

$$XY = A,$$

where X is the length of the specimen in the compression direction, Y the length in the extension direction and A is the surface area of the model.

Partially differentiate with respect to time:

$$X\,\partial Y/\partial t + Y\,\partial X/\partial t = \partial A/\partial t$$
$$\partial Y/\partial t = (1/X)(\partial A/\partial t) - (Y/X)(\partial X/\partial t).$$

Here $\partial X/\partial t$ and $\partial Y/\partial t$ are clearly the displacement rates of the compression and extension pistons.

For small changes in volume, the relationship between pressure change and volume change can be approximated as:

$$\partial P = K\,\partial V/V$$
$$= K\,\partial A/A \text{ for plane strain,}$$

where K is a constant, P the pressure and V the volume. On rearrangement, this gives:

$$\partial A = A\,\partial P/K$$
$$= XY\,\partial P/K.$$

Now, substituting in the previous equation for the required displacement rate of the extension piston gives:

$$\partial Y/\partial t = (1/X)(XY/K)(\partial P/\partial t) - (Y/X)(\partial X/\partial t)$$
$$= (Y/K)(\partial P/\partial t) - (Y/X)(\partial X/\partial t)$$
$$\text{'correction'} \quad \text{'strain rate component'}.$$

In practice, the values of $\partial X/\partial t$ (the current displacement rate of the compression piston), X, Y, P_r (the required stress on the side plate) and P_a (the actual, measured side stress) are known at each sampling instant. The compressibility constant K is a calibrated value for the particular modelling material. The control program then determines the necessary correction to the displacement rate of the extension piston using $\partial P/\partial t = (P_r - P_a)/4T_d$, where T_d is the time interval between sampling events. In other words, it tries to correct the discrepancy between actual and required values over the next four sampling intervals, employing a similar damping technique to that for strain rate control.